A New Scalable Model for Spiral Inductors on Lossy Silicon Substrate

Daniel Melendy** and Andreas Weisshaar*
**National Semiconductor Corporation
Santa Clara, CA 95052
* Department of Electrical and Computer Engineering
Oregon State University
Corvallis OR 97331-3211

Abstract— **A new scalable, predictive model for spiral inductors on lossy silicon substrates for radio-frequency integrated circuits (RFICs) is presented. The model is based on an enhanced Partial Element Equivalent Circuit (PEEC) approach. Eddy-current losses in the substrate are efficiently modeled using a complex image approach combined with available closed-form equations for partial inductance. The model further includes the conductor skin and proximity effects through discretization of the spiral segments. The resulting enhanced PEEC model is used to predict the performance of a typical 3.5 turn, 2.0nH octagonal spiral inductor fabricated in a heavily-doped BiCMOS process. Comparison with measurements over a 100 MHz to 10 GHz frequency range demonstrates excellent accuracy of the new modeling approach.**

I. Introduction

Scalable modeling of monolithic spiral inductors in radio-frequency integrated circuits (RFICs) is, in general, a complex electromagnetic problem. To predict the frequency-dependent characteristics of a spiral inductor with arbitrary geometry and substrate parameters, several complicated loss effects must be accurately modeled. For inductors built on low-loss substrates, such as GaAs, the quality factor (Q) is limited by the resistance of the metalization as well as the conductor skin and proximity effects. Spiral inductors fabricated on silicon additionally suffer from losses associated with the resistive nature of the substrate. In particular for inductors over heavily-doped silicon substrates with bulk resistivities on the order of 0.01Ω·cm, the time-varying magnetic field can result in significant inductor losses through the creation of eddy-currents in the conductive silicon.

Often, designers must rely on full-wave 3-D electromagnetic field solvers to accurately predict the Q or inductance of spiral inductors on lossy silicon substrate. Unfortunately, these simulations usually require large amounts of computational time and system memory. As an alternative, quasi-static methods have been developed which can reduce computational demands. In particular, the Partial Element Equivalent Circuit (PEEC) technique [1]-[3] has recently gained much popularity as a means for modeling spiral inductors. This popularity is largely due to the inherent flexibility of the PEEC approach to model various spiral inductor geometries and configurations. The major drawback of the traditional PEEC approach is the necessity of discretizing all conductive portions of a particular problem space. This technique is especially inefficient when modelling spiral inductors on highly doped silicon substrates.

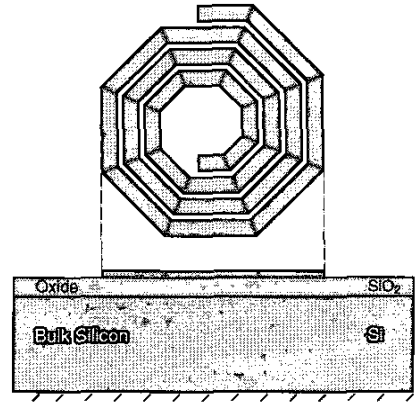

Fig. 1. Typical multi-turn octagonal spiral inductor fabricated on a lossy silicon substrate.

In this paper, the traditional PEEC approach is extended to efficiently include losses due to eddy-currents in lossy silicon substrate. This enhancement is based on a combination of closed-form equations for partial inductance and a complex-image technique [4]. The new scalable model is applied to a 2.0nH octagonal spiral inductor fabricated on a heavily-doped BiCMOS process, with the results showing excellent agreement to measurement data.

II. PEEC Modelling of Spiral Inductors

In general, PEEC models are composed of ideal "partial" components, such as partial inductances, partial resistances, etc. These components can be calculated through a variety of closed-form equations and quasi-static techniques, [5] - [8]. The number of partial components is directly determined by the level of discretization of the problem space. For spiral inductor footprints

0-7803-7695-1/03/$17.00 © 2003 IEEE

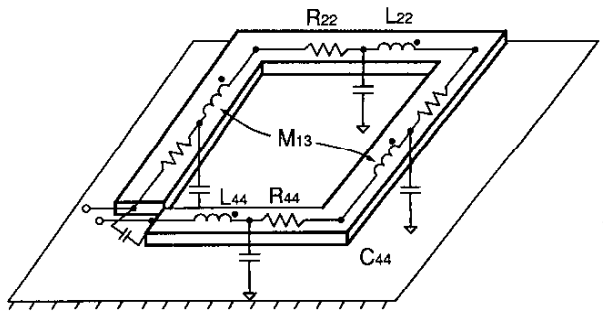

Fig. 2. PEEC model for single turn rectangular spiral inductor suspended above a perfect ground plane.

on the order of $300\mu m^2$, in the DC to 10 GHz frequency region, it is usually sufficient to discretize on a segment-by-segment basis along the length of the spiral inductor, [9]. Often, to obtain wide-band accuracy, it is also necessary to discretize each segment into multiple parallel filaments to properly model the conductor-skin and proximity effects, [10]. This results in multiple, parallel R-L circuit branches between the nodes of the equivalent circuit.

Figure 2 shows and example of a single turn rectangular spiral inductor and superimposed the corresponding PEEC model. The lossy silicon has been temporarily replaced with free-space to simplify the problem. In this case, the spiral inductor is divided into four separate conductor segments, each with a partial inductance and resistance. Each parallel segment pair is also linked with a partial mutual inductance. It should be noted that the values of the self- and mutual-inductances must take into account the ground plane below the spiral inductor. The capacitive coupling between each of the conductor segments and the ground plane has also been included through the addition of partial self-capacitances of each segment. For multi-turn spiral inductors, partial mutual capacitances should be included between adjacent segments for improved accuracy.

To solve the more practical problem of a spiral inductor on lossy silicon substrate using the traditional PEEC approach, a large volume of the bulk silicon below the spiral inductor must be discretized and included in the equivalent circuit. This impractical approach is necessary to accurately model the shunt and eddy-current losses occurring in the silicon substrate. The resulting equivalent circuit is not only time-consuming to assemble, but prohibitive in size.

III. Complex Image Technique

In [11], [4] a 2-D quasi-magnetostatic assumption is used to find the Green's function for a line-current above a lossy silicon substrate with a ground plane. The result indicates that the lossy silicon substrate can be approximately replaced by a perfect ground plane at an

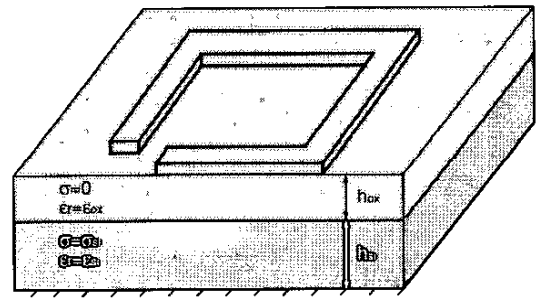

Fig. 3. Single turn rectangular spiral inductor on standard Si-SiO_2 substrate.

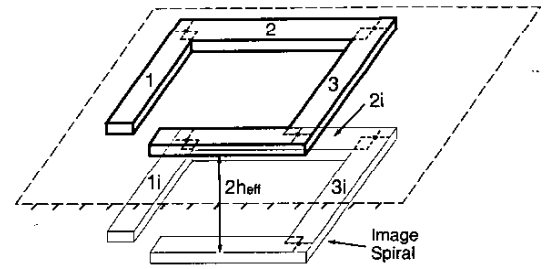

Fig. 4. Complex image spiral replacing the lossy substrate.

effective complex distance, h_{eff}, below the line current. For a standard Si-SiO_2 substrate, h_{eff} is given as [4]

$$h_{\text{eff}} = h_{\text{ox}} + \frac{1-j}{2}\delta_{\text{si}} \tanh\left(\frac{(1+j)h_{\text{si}}}{\delta_{\text{si}}}\right) \qquad (1)$$

where h_{ox} is the oxide thickness, h_{si} is the bulk thickness, and δ_{si} is the skin depth of the bulk silicon. The skin depth of the bulk silicon is given by

$$\delta_{\text{si}} = \frac{1}{\sqrt{\pi f \mu_0 \sigma_{\text{si}}}} \qquad (2)$$

It is important to note that the combination of (1) and (2) indicate that h_{eff} is frequency- and process-dependent.

This technique can be directly applied to the PEEC methodology for modeling monolithic spiral inductors on lossy silicon substrates. Specifically, for the single-turn spiral inductor illustrated in Figure 3, a basic PEEC model can be developed by sub-dividing the physical spiral into four separate conductor segments. Applying the complex-image technique described above, the lossy substrate would then be replaced by a perfect ground plane at a complex distance, h_{eff}, below the four segments. Further, using the method of images, the perfect ground-plane can be replaced by an image of the spiral inductor at a distance $2 \cdot h_{\text{eff}}$ below the physical spiral inductor as demonstrated in Figure 4.

To calculate the total self-inductance for a particular segment, it is necessary to combine the free-space and

image partial inductances. For example, to find the total partial self-inductance of segment 1, the equal and opposite current in image segment 1i must be taken into account,

$$L_{1,\text{total}} = L_{1,\text{free-space}} - M_{1,1i} \tag{3}$$

where $M_{1,1i}$ is calculated using the complex distance between segment 1 and 1i. The resulting total partial self-inductance for segment 1 becomes complex and frequency-dependent.

In general, for a spiral inductor over a perfect ground plane, the branch partial inductance matrix, [10], for the N coupled segments in the PEEC model can be summarized as

$$\mathbf{L}_{\text{total}}^{(N\times N)} = \mathbf{L}_{\text{free-space}} - \mathbf{L}_{\text{image}} \tag{4}$$

where $\mathbf{L}_{\text{free-space}}$ contains partial self- and mutual-inductances for physical segments and $\mathbf{L}_{\text{image}}$ contains partial mutual inductances between the physical segments and their images exclusively. Due to the complex, frequency-dependent distance, $2h_{\text{eff}}$, between the spiral inductor and its image, it can be expected that $\mathbf{L}_{\text{image}}$, and consequently $\mathbf{L}_{\text{total}}$, will also be complex and frequency dependent. This complex inductance can be interpreted using the following relationships

$$\mathbf{L}(\omega)_{\text{total}} = Re\left(\mathbf{L}(h_{\text{eff}})_{\text{total}}\right) \tag{5}$$

and

$$\mathbf{R}(\omega)_{\text{total}} = -\omega Im\left(\mathbf{L}(h_{\text{eff}})_{\text{total}}\right) + \mathbf{R}_{\text{DC}} \tag{6}$$

where $\mathbf{L}(\omega)_{total}$ contains the frequency-dependent total partial inductances and $\mathbf{R}(\omega)$ contains partial resistances due to the ohmic losses from eddy-currents in the substrate as well as the DC resistances of the conductors. In general, $\mathbf{R}(\omega)_{\text{total}}$ will contain mutual partial resistances as well as the usual self partial resistances. These mutual resistances can be attributed to ohmic losses in the shared return paths for separate segments.

It is important to note that the resulting enhanced-PEEC model is assembled from frequency-dependent components. This limits the approach to providing frequency domain information, as opposed to traditional PEEC models which are valid in both the time- and frequency-domains. In [12], a wide-band compact equivalent circuit model is described, which is extracted from the frequency domain information and is suitable for use in time- and frequency-domain simulations.

IV. Results

A 2.0nH octagonal spiral inductor on a high-loss epi-substrate was chosen to demonstrate the usefulness of the enhanced-PEEC scalable-model. This spiral inductor was fabricated with 3.5 turns on a BiCMOS process with bulk and epi-layer conductivities of approximately

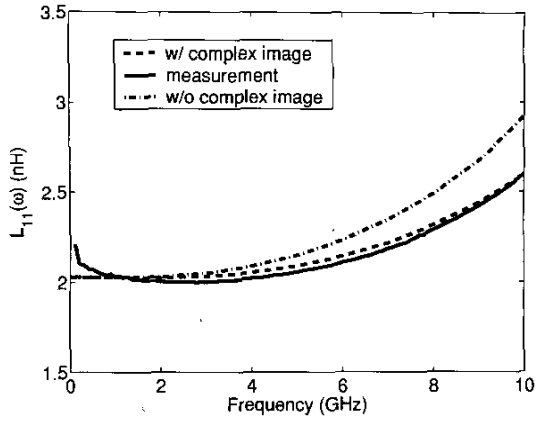

Fig. 5. Measured total inductance for 2.0nH octagonal spiral inductor versus scalable model results.

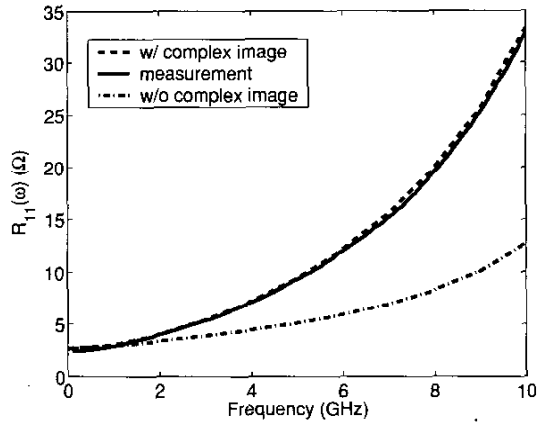

Fig. 6. Measured total resistance for 2.0nH octagonal spiral inductor versus with scalable model results.

10^4 S/m and 10 S/m, respectively. The high conductivity of the bulk silicon indicates that eddy currents will have a strong effect on the performance of the spiral inductor. The underpass is fabricated in the next metal layer below the inductor. In this case, the PEEC model was configured to have 7 filaments in the width direction and 4 filaments in the height direction of each segment.

The resulting one-port inductance is shown in Fig. 5 along with measurements. Two separate results from the scalable model are plotted, one with the complex-image approach used, the other without. For the case without the complex-image, the total inductances were calculated for the real conductors plus the *real* images due to the ground plane at the backside of the silicon substrate. For frequencies less than 4 GHz, this approximation gives reasonable results. However, above 4 GHz, the eddy currents in the substrate cause a significant lowering of the total inductance and increase in resistance (loss).

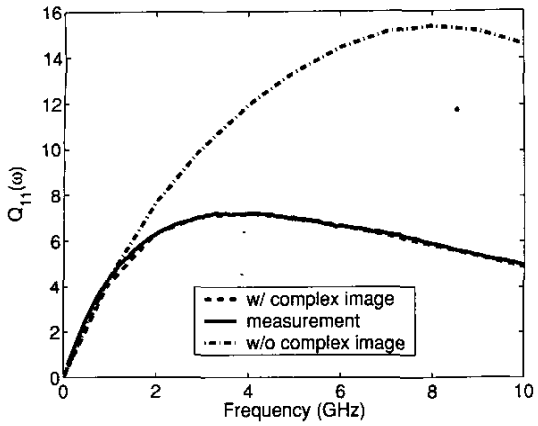

Fig. 7. Measured total quality factor for 2.0nH octagonal spiral inductor versus scalable model results.

Figure 6 shows the measured one-port resistance of the spiral inductance along with the results from the scalable model. In this case, by ignoring the eddy-currents, the total resistance is more than 60% below the measured value. This increase in resistance can be attributed to ohmic losses generated by the eddy-currents in the substrate.

The measured one-port Q, Q_{11}, of the 2.0nH spiral is shown in Fig. 7 along with predicted results from the scalable model. By including the substrate losses with the complex-image technique, the scalable model is able to accurately predict the Q peak of 7.2 at approximately 4GHz. The results with and without complex image further suggest an over 100% increase in peak Q for low resistivity bulk silicon.

V. Conclusion

A scalable, predictive model for spiral inductors on highly doped silicon substrate was presented. The new model combines a complex-image technique with the traditional PEEC approach to efficiently include eddy-current losses affecting spirals on high-loss silicon. This flexible approach can provide accurate frequency-domain information such as $Q_{11}(\omega)$, $L_{11}(\omega)$, or $R_{11}(\omega)$ over a DC to 10 GHz frequency range for a variety of spiral geometries and substrate configurations.

Results were presented for a 2.0nH octagonal spiral on a high-loss silicon epi substrate where eddy-current losses can be expected to dominate. The comparison with measurements showed that the enhanced-PEEC model is accurate over the 100 MHz to 10 GHz frequency range. In particular, the scalable model was able to accurately predict the peak Q of 7.2 at 4 GHz.

Acknowledgment

This research was supported in part by the NSF Center for the Design of Analog and Digital Integrated Circuits (CDADIC).

References

[1] A.E. Ruehli, "Equivalent Circuit Models for Three-Dimensional Multiconductor Systems," *IEEE Trans. Microwave Theory Tech.*, vol. 22, pp.216–221, March 1974.

[2] A.M. Niknejad and R.G. Meyer, *Design, Simulation, and Applications of Inductors and Transformers for Si RF ICs.* Kluwer Academic Publ., 2000.

[3] R.D. Lutz, et al., "Modeling and analysis of multilevel spiral inductors for RFICs," *IEEE MTT-S International Microwave Symposium Digest*, vol. 1, pp. 43–46, 1999.

[4] A. Weisshaar, H. Lan, and A. Luoh, "Accurate Closed-Form Expressions for the Frequency-Dependent Line Parameters of Coupled On-Chip Interconnects on Lossy Silicon Substrate," *IEEE Trans. Adv. Packaging*, vol. 25, No. 2, pp. 288–296, May 2002.

[5] C. Hoer and C. Love, "Exact Inductance Equations for Rectangular Conductors With Applications to More Complicated Geometris," *J. Research, National Bureau of Standards–C. Engineering and Instrumentation*, Vol. 69C, No. 2, pp.127–137, April-June 1965.

[6] F.W. Grover, *Inductance Calculations, Working Formulas and Tables.* D. Van Nostrand Company, Inc., 1946.

[7] R. Gharpurcy, "Modeling and Analysis of Substrate Coupling in Integrated Circuits," *PhD Dissertation,* Department of Electrical Engineering and Computer Sciences, University of California at Berkeley, 1995.

[8] K. Nabors and J. White, "FastCap: A Multipole Accelerated 3-D Capacitance Extraction Program," *IEEE Trans. Computer Aided Design*, vol. 10, pp. 1447–1459, Feb. 1973.

[9] D. Melendy, "Modelling of On-Chip Spiral Inductors for Silicon RFICs," *Masters Thesis,* Department of Electrical and Computer Engineering, Oregon State University, Nov. 2002.

[10] M. Kamon et al., "FASTHENRY: A Multipole-Accelerated 3-D Inductance Extraction Program," *IEEE Trans. Microwave Theory Tech.*, vol. 42, pp. 1750–1758, Sept. 1994.

[11] A. Weisshaar and H. Lan, "Accurate Closed-Form Expressions for the Frequency-Dependent Line Parameters of On-Chip Interconnects on Lossy Silicon Substrate," *IEEE MTT-S International Microwave Symposium Digest*, pp. 1735–1756, Phoenix, Arizona, May 20-25, 2001.

[12] D. Melendy, P. Francis, C. Pichler, K. Hwang, G. Srinivasan, and A. Weisshaar, "A New Wide-Band Compact Model for Spiral Inductors in RFICs," *IEEE Electron Device Lett.*, vol. 23, pp. 273–275, May 2002.